

Dokumentutgivare

Lunds Universitet

Handläggare

Klas Malmqvist

Författare

Dokumentnamn
rapport

Utgivningsdatum

21/8 1981

Dokumentbeteckning

LUTFD2/TFKF-3027/(1981)

Ärendebeteckning

Klas G Malmqvist, Gerd I Johansson och K. Roland Akselsson
Inst för kärnfysik, LTH, Sölvegatan 14, 223 62 LUND

Dokumenttitel och undertitel

A facility for multielemental analysis by PIXE and the $^{19}\text{F}(p,\alpha\gamma)^{16}\text{O}$ reaction

Referat (sammandrag)

Specific advantages with Particle Induced X-Ray Emission are: its 1) multielemental capability, especially when combined with nuclear techniques for lighter elements, 2) speed, 3) low detection limits for small samples and 4) accuracy. To make full use of these advantages, analytical parameters have to be chosen optimally and the facility to be carefully designed. This paper describes an experimental facility constructed to permit continuous development work to optimize the analytical conditions and to allow the gradual implementation of automatic control. Emphasis is also put on the simultaneous use of proton induced gamma rays from fluorine. The features and the performance of the set-up including its accuracy, precision and experimental detection limits are reported.

Referat skrivet av

Författarna

Förslag till ytterligare nyckelord

Klassifikationssystem och -klass(er)

Indextermer (ange källa)

Omfång

29

Ovriga bibliografiska uppgifter

Språk

Eng

Sekretessuppgifter

ISSN

ISBN

Dokumentet kan erhållas från

Mottagarens uppgifter

Författarnas adress ovan

Pris

gratis

Blankett LU 11:25 1976-07

SIS
DB 1

DOKUMENTDATABLAD enligt SIS 62 10 12

A FACILITY FOR MULTIELEMENTAL ANALYSIS BY PIXE AND THE $^{19}\text{F}(p,\alpha\gamma)^{16}\text{O}$ REACTION

Klas G. Malmqvist, Gerd I. Johansson and K. Roland Akselsson

Department of Nuclear Physics, Lund Institute of Technology
Sölvegatan 14, S-223 62 LUND, SWEDEN.

Specific advantages with Particle Induced X-Ray Emission are: its 1) multielemental capability, especially when combined with nuclear techniques for lighter elements, 2) speed, 3) low detection limits for small samples and 4) accuracy. To make full use of these advantages, analytical parameters have to be chosen optimally and the facility to be carefully designed. This paper describes an experimental facility constructed to permit continuous development work to optimize the analytical conditions and to allow the gradual implementation of automatic control. Emphasis is also put on the simultaneous use of proton induced gamma rays from fluorine. The features and the performance of the set-up including its accuracy, precision and experimental detection limits are reported.

INTRODUCTION

Particle Induced X-Ray Emission, PIXE, has been a rapidly developing analytical technique over the last decade. Since 1970, when Johansson et al presented their pioneering paper,¹ PIXE has been applied in many different fields of science, e.g. atmospheric chemistry and medicine. Two International Conferences on Particle Induced X-Ray Emission and its Analytical Applications held at Lund in 1976 and 1980 have clearly demonstrated this development^{2,3}.

To make extensive use of the specific advantages of PIXE, e.g. multielemental capability, speed, low detection limits for small samples and accuracy, appropriate experimental arrangements and procedures have to be developed.

As compared to other X-ray techniques, one of the major advantages of PIXE is the possibility of simultaneously using the information carried by nuclear reaction products including the scattered projectile particles and hence extending its analytical capability also to elements lighter than sulphur. The feasibility of using Particle Elastic Scattering Analysis (PESA) has been shown

at several laboratories^{4,5}. Most PIXE-laboratories, however, use 2-4 MeV protons which limits the usefulness of PESA to the analysis of major (light) constituents and to the determination of total sample mass⁶. The gamma rays from nuclear reactions are the other possible source of information on light elements. The advantages of using such gamma rays have been demonstrated in several articles^{7,8}.

Due to its high abundance in some common welding rods, fluorine may be found in high concentrations in air in work places, being sometimes the first element to exceed its hygienic threshold limit value. Particular interest in the characterization of welding aerosols at our laboratory⁹ has initiated the development of a procedure for analysing fluorine using the $^{19}\text{F}(p,\alpha\gamma)^{16}\text{O}$ reaction simultaneously with PIXE.

For studies of the fluorine depth distribution in various matrices the $^{19}\text{F}(p,\alpha\gamma)^{16}\text{O}$ reaction has been used extensively, making use of the resonance character of the cross section^{10,11}. In order to obtain the total mass of fluorine in samples of thicknesses from 0.1 to 1 mg/cm², e.g. in an aerosol sample on a filter from a work place investigation, it is necessary to have a yield of gamma rays per fluorine atom which is almost independent of the depth in the sample. As will be further discussed, protons with energies of about 2.5 MeV, which fortunately is also an energy well suited for PIXE analysis, can be used for this kind of analysis.

The design of the experimental set-up is crucial for optimal use of the speed, the low detection limits and the accuracy of PIXE. To facilitate continuous optimization, the set-up is characterized by flexibility and prepared for automatic control. This has been achieved at the price of increased complexity which introduces some extra concern about charge integration.

In this paper, the system for PIXE and fluorine analysis and its performance are described.

THE PIXE FACILITY

Basic design

The vacuum chamber of this facility for combined X-ray and gamma ray analysis is

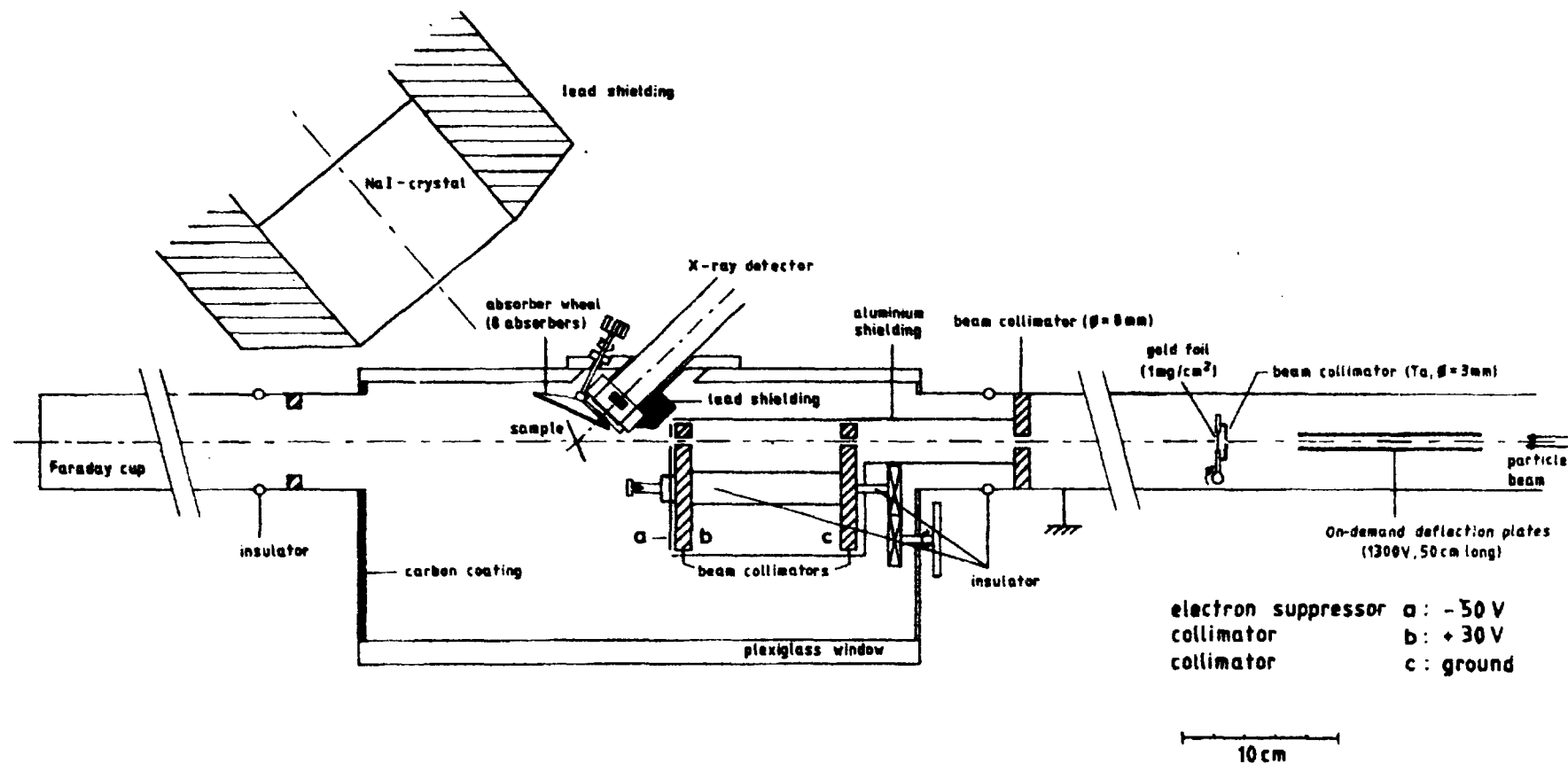


Fig. 1. Irradiation chamber for simultaneous X-ray and gamma ray analysis.

is shown in fig. 1. The size and shape of the chamber are partly determined by the demands for flexibility mentioned above. It is constructed from stainless steel and partly covered on the inside with carbon plates to reduce the characteristic X-ray background caused by scattered protons. On the top and the front walls exchangeable plexiglass windows allow observation of the interior parts. A "revolver" including ten sets of circular carbon collimators (table 1), each set consisting of a pair of collimators separated by 10 cm, allows the selection of a proper beam diameter from outside the chamber. The choice of beam diameter depends on the type of sample and the specific analytical task. Between the target and the last collimator a secondary electron suppressor ($U = -50$ V) is inserted to prevent the escape of electrons from the charge measurement region. The collimator revolver is shielded from the irradiation chamber by a grounded aluminium foil. In order to achieve a proton beam with a constant intensity distribution over its entire cross section, the beam is passed through a thin gold foil (1 mg/cm^2 , gold evaporated on to glass plates and then floated off on water and fixed to a frame) situated 0.6 m before the target. This foil represents a compromise between having a homogeneous beam at the target and the consequent reduction in beam intensity (about a 15-fold reduction for 8 mm beam diameter). Since with this beam diameter it is anyhow possible to obtain a current of 200 nA at the target, this intensity reduction does not represent a severe limitation.

A Si(Li)-detector (Kevax, sensitive area: 80 mm^2 , crystal thickness: 5 mm; resolution: 158 eV at 5.9 keV) is inserted into the chamber wall, at 135° relative to the beam (which gives a lower intensity of electron bremsstrahlung than at 90° , ref.¹²) with a distance of 0.040 m between the target and crystal. To maintain vacuum (better than 10^{-4} torr) but allow low energy X-rays to leave the chamber, a window (110 μm beryllium) is attached between the detector window (25 μm beryllium) and the target. The large variety of analytical situations places considerable demands on a proper choice of X-ray absorber and hence a wheel fitted with 8 different X-ray filters (see table 1) allows the insertion of an absorber suitable for the specific analytical situation. A stainless steel compartment beneath the chamber, designed for the $5 \times 5 \text{ cm}^2$ standard photographic slide frames which are commonly used at many PIXE laboratories, contains a slide tray taking 40 samples. This compartment is evacuated before the valve, separating the container from the chamber, is opened, thus minimizing the time wasted due to pumping. By electro-pneumatic remote control, a sample is positioned in the proton beam and after analysis automatically replaced by using computer steering. The sample changing procedure can be checked over a closed-circuit television network.

Table 1

Beam collimators: diameters (mm) : 1, 3, 4, 5, 7, 8, 9, 10, 12

X-Ray absorbers:

<u>material</u>	<u>thickness (um)</u>	<u>hole (%)</u>
Mylar	77	—
Mylar	340	—
Mylar	340	1.66
plexiglass	1110	—
aluminium	53	0.12
aluminium	152	—
aluminium	154	1.78
aluminium	310	(x)

(x) Double layer absorber made from two 155 μm aluminium foils, one with 4.3% and one with 0.06% relative hole areas. The foils are put together with coaxial holes. This absorber is specially designed for the analysis of geological material⁸.

Table 1. Diameters of the beam collimators and specifications of the X-ray absorbers which can be selected in the set-up discussed.

With a sample in position for analysis, the sample mounting frame (aluminium) automatically makes electrical contact with the chamber. This facilitates the charge transport, especially from thick samples, thus reducing the risk of charge build-up. However, for highly insulating thick samples, local positive voltages may reach several tens of kilovolts before electrical discharges occur and due to the acceleration of electrons towards the positively charged sample, a significantly increased electron bremsstrahlung background will occur in the X-ray spectrum. To avoid this, a battery operated carbon filament is used to spray the sample with electrons¹³. The use of a closed battery circuit prevents the introduction of false currents which might spoil the current integration. The latter is made using a current digitizer (ORTEC 439) and a scaler to count the number of charge pulses. For very low currents ($< 2 \text{ nA}$), special precautions are necessary so as not to disturb the current measurement. No one is allowed to move close to the set-up, since changes in the chamber capacitance may be

induced. Further careful grounding of surrounding equipments and electronics is required to reduce induction of currents.

X-rays produced in the sample by proton (2.55 MeV) bombardment are detected in the Si(Li) crystal producing signals which after passing a preamplifier enter an X-ray amplifier (Kevex 4525P) and a fast leading edge discriminating system (ORTEC 474 + ORTEC 406A). Pulses from this system trigger an on-demand beam deflection device¹⁴. About 400 ns after the detection of an X-ray event an electron tube (PL 519) grounds one of two parallel plates, normally kept at 1300 V and situated about 0.7 m up the beam line. The sudden electric field between the two plates deflects the proton beam from the target and keep it off while the X-ray amplifier is busy processing the X-ray event (for an 8 μ s amplifier time constant the processing time is approximately 80 μ s). Due to this on-demand beam system, radiation damage, sample heating and pulse pile-up are reduced and the electronic dead-time is insignificant. The system is routinely operated together with the electronic pulse pile-up rejector of the X-ray amplifier to reject any events arriving while the beam is off.

After shaping and stretching in the X-ray amplifier, the pulse is fed to an analog-to-digital converter and then stored in a computerized multichannel analyzer (Nuclear Data 6620). The spectrum evaluation is done with the HEX computer code¹⁵ comprising non-linear least squares fitting. To improve the accuracy and to allow for the use of high count rates (up to 5000 cps), the code has been implemented with corrections for Si-escape peaks and pile-up peaks¹⁶.

The system calibration for quantitative PIXE analysis¹⁷ is determined by the repeated irradiation of 45 homogeneous single element standard foils of accurately known elemental masses (the accuracy of individual foils is stated to be better than 5%, ref.¹⁸). Careful measurements or estimations of physical parameters, e.g. sample-to-detector distance, detector crystal dead-layer thickness etc., are used to attain an initial calibration. A calibration curve is fitted to the measured elemental yields with special attention to the physical interpretation and by comparing it with the estimated initial calibration. This procedure is then repeated iteratively.

To determine the accurate thicknesses of the X-ray absorbers, they are calibrated by analysing suitable homogeneous samples with and without the respective absorbers. For absorbers with hole (to transmit part of the low energy X-rays), the solid angle of the holes are determined by irradiation of a

low-Z element sample with and without the absorbers. The efficient beam area of each collimator is determined by analysing a spot-sample of accurately known elemental mass. For further details regarding the calibration procedure, refer to ref.¹⁸.

The requirements for high sample processing rates are taken care of by preparing the set-up for computer control. At present, sample changing is made automatically and both beam collimators and X-ray absorbers are designed for remote control via stepping motor drives.

Charge measurement

The number of protons incident on the target is integrated by use of a current digitizer and to check its accuracy, a high impedance ($R_i = 1000$ megaohms) voltmeter was used to measure the voltage over a 10 megaohms precision resistor (inaccuracy below 0.1%). For currents higher than 10 nA the inaccuracy of the digitizer is below 0.5 % and for currents between 1 and 10 nA below 1 %. Hence, even at low beam currents, the inaccuracy of the digitizer will be insignificant.

The current integrator is normally connected to the irradiation chamber as well as to the Faraday cup. Measurements show that for 2.55 MeV protons in this special set-up and for the total thickness of sample and substrate exceeding 3 mg/cm² it is necessary to collect the charge from the chamber as well as that from the Faraday cup. Unless this is done systematically a low charge will be measured, due to scattering of particles in the sample.

When striking the target, the protons will produce secondary electrons and some of those produced near to the surface of the material are emitted from the sample. The relative yield of such electrons will depend on proton energy and sample composition¹⁹. The total charge of these electrons has to be measured for accurate charge integration. To avoid the escape of the electrons through the last collimator, a negatively biased electron suppressor is inserted between it and the sample. In fig.2 the number of K X-rays per measured charge from an infinitely thick silver plate is plotted versus the negative bias of this suppressor. From the plot it can be inferred that at least -20 V is required in this special arrangement for accurate charge integration (the bias normally used is -50 V).

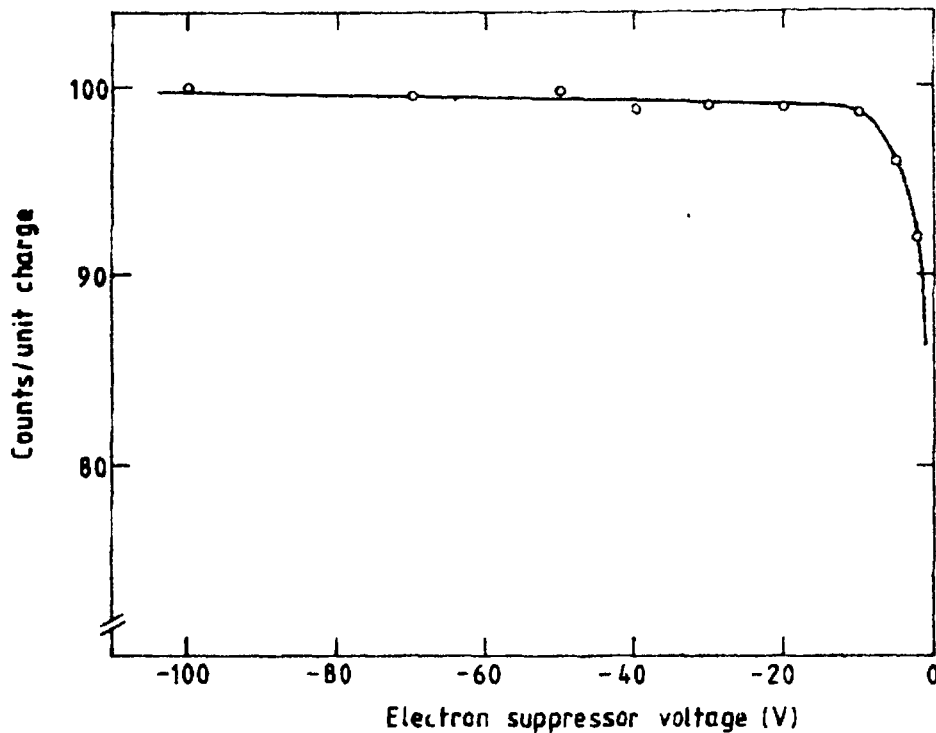


Fig. 2. Numbers of Ag K X-rays per measured charge (arbitrary units) from a thick silver plate plotted versus the negative bias on the electron suppressor. The proton current was 2 nA.

Due to the scattering of protons in the first collimator, some protons will hit the second collimator although this has a slightly larger diameter than the first one. To keep the secondary electrons produced in the last collimator from reaching the region of charge collection, it is kept at a positive voltage (+30V, empirically determined).

For accurate results the number of X-rays per unit charge should remain constant for different proton currents. To check for this, samples were analysed with varying currents and in fig.3 the number of Cu K X-rays per measured charge are plotted versus current for an infinitely-thick carbon pellet.

Since very low proton currents (1 to 5 nA) are occasionally used, the analysis will be very sensitive to erroneous extra currents. The on-demand beam system¹⁴ uses an electron tube for rapid grounding of one of the deflection plates. This system is a strong emitter of electromagnetic radiation, which may be picked up by parts of the current measurement system, thereby inducing extra currents in the nanoampere range. This can be checked with no beam on the target and an X-ray source on the detector to simulate normal count rates in the beam

deflection system. To avoid such currents, only coaxial cables are used and their shields are connected to ground at several points. There may also be other reasons for additional currents and this is an important problem worth much attention from any user of large irradiation chambers anxious to perform accurate ion beam analysis.

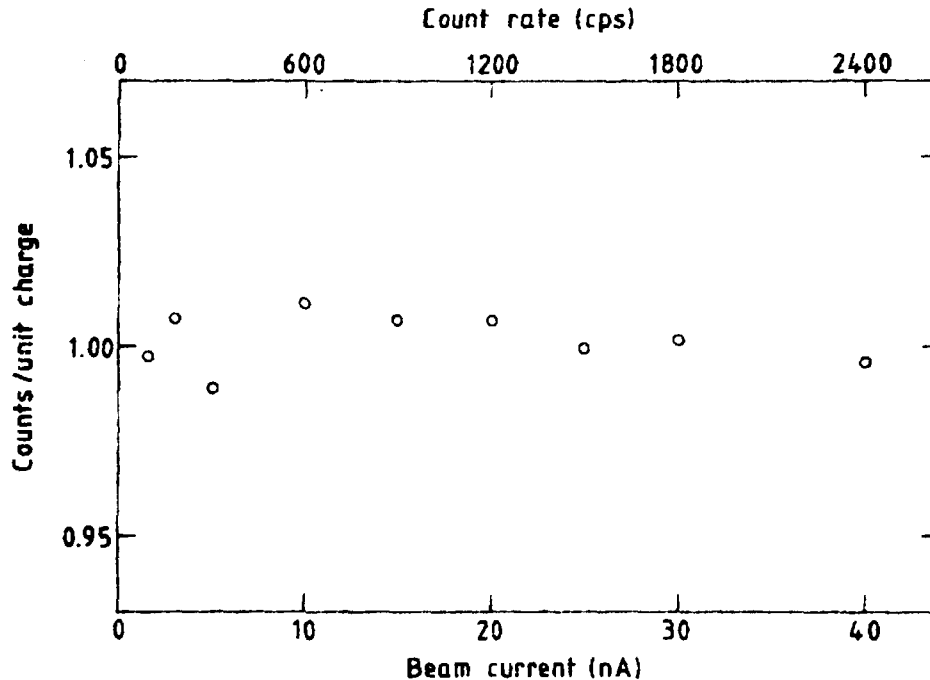


Fig. 3. Numbers of Cu K X-rays per unit charge (arbitrary units) versus proton beam current and count rate, when bombarding an infinitely thick carbon pellet. The statistical uncertainty in each determination is less than 1%.

Proton beam performance

The homogeneous current density over the beam cross section required for the analysis of small inhomogeneous samples is obtained by a diffuser foil. Such an arrangement causes a significant reduction in beam intensity as compared to the use of the electrostatic proton beam sweeping technique. The latter, however, has at least one significant disadvantage for the analysis of inhomogeneous samples: a well focussed beam of high intensity, swept at a kilohertz frequency over the sample, may induce a rather low average count rate, but can intermittently give rise to high rates. Since the probability for pulse pile-up

is proportional to the square of the instantaneous count rate, possible high local concentrations of elements present in an inhomogeneous sample will, in case of proton beam sweeping, cause enhanced pulse pile-up in the spectrum.

To check the beam homogeneity, the beam mapping method²⁰ has been applied. First, the beam is focussed and steered through the sample centre and then a diffuser foil (gold foil; 1 mg/cm²) preceded by a small tantalum collimator (diameter: 3 mm) is inserted into the beam. To be able to reproduce its position, horizontal and vertical micrometer gauges are used. A small piece of copper foil was fixed to a polymer foil (Kapton, thickness 7.5 μ m) and moved horizontally and vertically stepwise in the plane of the sample through the beam with an 8 mm diameter. The number of X-rays (Cu K _{α}) was registered and normalized to the beam charge collected. In fig. 4a is shown the beam intensity distribution in the vertical direction.

For small samples, e.g. impactor samples, the measured numbers of X-rays will vary with their horizontal positions in the homogeneous beam because of the varying solid angle relative to the detector. In this case it is feasible to use a skew beam intensity profile with lower intensity at the side closer to the detector. In fig 4b. the horizontal beam intensity distribution has intentionally been made skew so that the measured number of X-rays is approximately constant. For comparison, the result of a beam scan with a homogeneous beam is also shown (broken line). This solid angle effect is still more pronounced when the X-ray detector is at right angles relative to the beam and with small distance between the sample and the detector. In these cases the solid angle changes relatively more with position for small samples. In the experimental set-up discussed here, a skew beam profile is used routinely.

The theory of multiple scattering by Meyer²¹ may be used for comparison with experiments and as a guide for designing a suitably-skew beam profile. Figure 4a shows very good agreement between theory and experiment.

The collimator pairs are made from carbon, the second one being somewhat larger than the first one so as to reduce the number of protons scattered out of the beam which would otherwise form a low intensity halo around the beam core. The use of the beam mapping method outside the the beam core shows that, for a beam diameter of 8 mm, the current density of the halo 2 mm from the edge of the core is less than 0.1% of the core density. To reduce this further, the collimators are at present being replaced by tantalum collimators of anti-scatter design²².

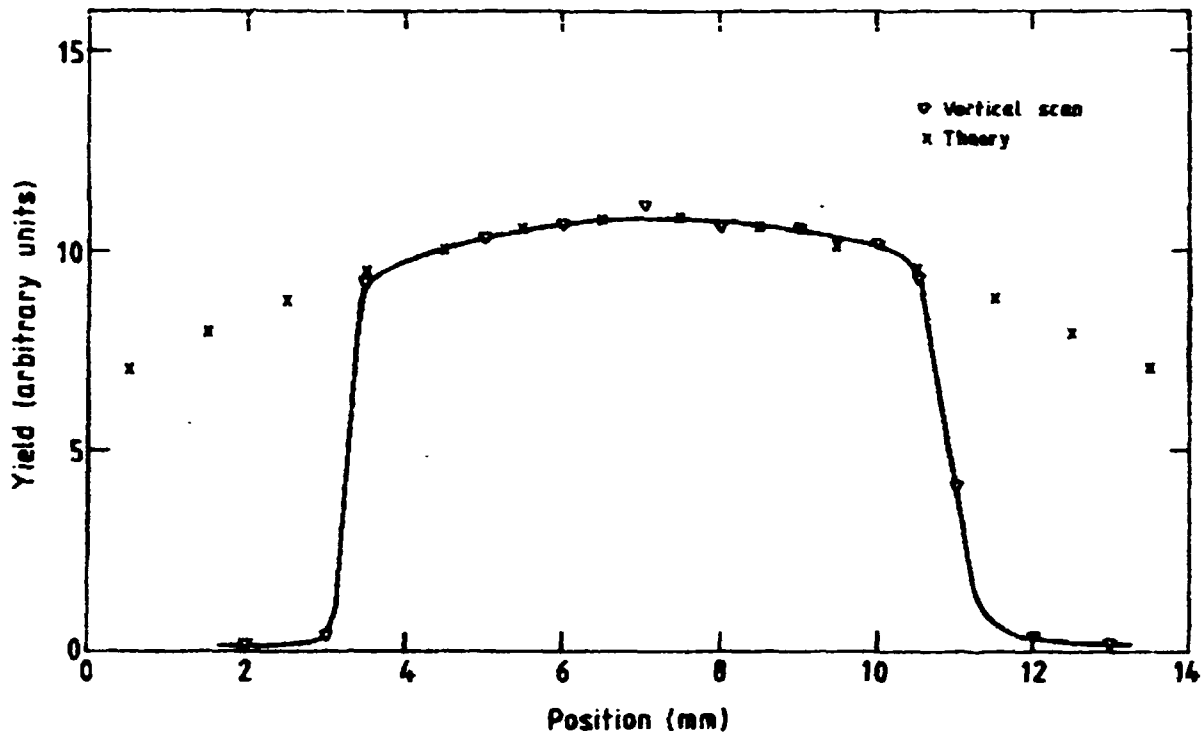


Fig. 4a. Experimental proton beam intensity profile in the horizontal (o) direction in the sample plane as measured by the beam mapping method²⁰. The beam collimator was 8 mm and the undiffused beam passed through the sample centre. For comparison, a theoretical profile based on the calculations by Meyer²¹ is also given (x).

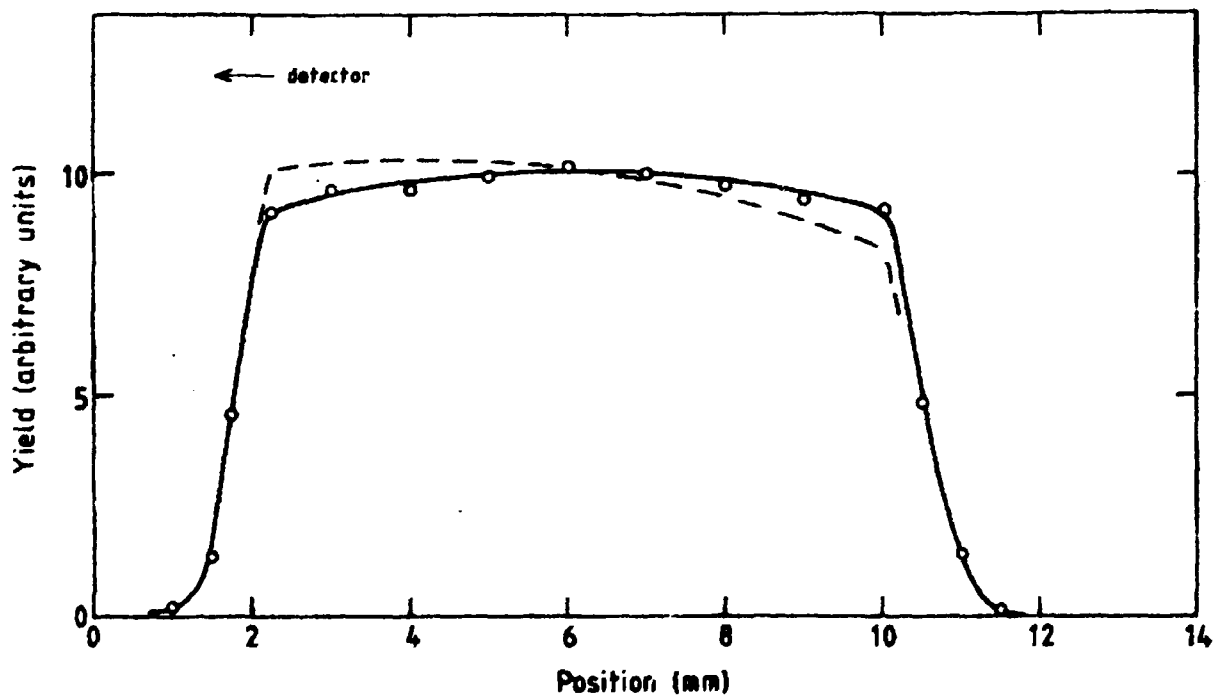


Fig. 4b. Horizontal beam scan for a skew beam intensity. The arrow points to the side closer to the detector. Small samples representing the same mass arbitrarily scattered over the beam cross section will in this case each yield approximately the same intensity. For comparison, a beam scan for a homogeneous beam is also given (broken line).

Detector effects

Particles scattered in the sample may, in cases when either none or a very thin X-ray absorber is used, reach the Si(Li) crystal with an energy of several hundreds of keV left. In such cases an event of very high energy is deposited in the detector. Frequent resets may occur in the optical feedback system of the preamplifier and severe distortions of the X-ray spectrum are obtained, e.g. peak broadening and peak centroid shift. Such effects render the X-ray spectra unsuitable for computer analysis and in severe cases may even render quantitative analysis impossible. This problem is avoided in the present set-up by using a beryllium foil of 110 μm thickness as window in the target chamber and thus still maintaining good transmission for low energy X-rays.

Similar distortions are also observed when bombarding certain kinds of targets, mainly those containing high concentrations of fluorine, e.g. aerosol filters made of Teflon fibres and some geological materials. The distortions are found even if a very thick absorber is used between the target and the detector. In these cases, high fluxes of gamma rays causes intermittent high (>1 MeV) energy depositions. This has been checked independently by analysing an X-ray spectrum and a gamma ray source (^{60}Co) simultaneously, obtaining the same kind of distortion of the X-ray peaks. Since the Si(Li) crystal cannot be shielded from gamma rays from the target position, samples producing an intense flux of high energy gamma rays have to be avoided. In some cases, it may be possible to select a proton energy having a low cross section for gamma ray production.

A significant background continuum in the X-ray spectrum is caused by gamma rays produced when the protons strike the collimators and then Compton scatter in the detector crystal^{2,3}. This yield is in particular significant when very thin targets with low intrinsic production of gamma rays are irradiated. By applying a lead shielding to the Si(Li) detector (see fig 1), the background for high X-ray energies is reduced by about 50% for 2.55 MeV protons and carbon collimators. By exchanging these for tantalum collimators, the background would be further reduced.

When X-rays are incident on the Si(Li) crystal close to the edge of the sensitive volume, incomplete charge collection may take place due to the distorted electric field pattern near the edge. As a result, the pulse height registered will be somewhat lower than the nominal pulse height from such an event. These degraded X-ray events form a low energy tail to the corresponding

full energy peak²⁴. This introduces difficulties in peak area determinations and an increased background for lower energy peaks riding on the tail. The effect can be reduced at the expense of reduced detector solid angle by inserting a collimator in front of the crystal and thereby preventing the X-rays from interacting in the poor electric field region.

The 80 mm² detector in this set-up is collimated to an approximate efficient sensitive area of 30 mm² by a tantalum collimator in front of the detector window. This reduces low energy tailing significantly as can be seen by comparing spectrum a and spectrum b in fig 5a. However, there is a significant residual tail which may cause slight problems in computer spectrum analysis. By bringing the detector bias to zero and then directly back again to its normal voltage (-1000 V) a significant decrease of peak tailing is achieved as can be seen in spectrum c in fig 5a. To check the time variation of the tailing after applying the detector bias, a ⁵⁵Fe-source was placed 10 mm in front of the detector (without collimation). The detector bias was applied and then pulse-height spectra were recorded after different times. In fig 5b the spectra are superposed, showing the gradual increase in peak tailing with time. When a

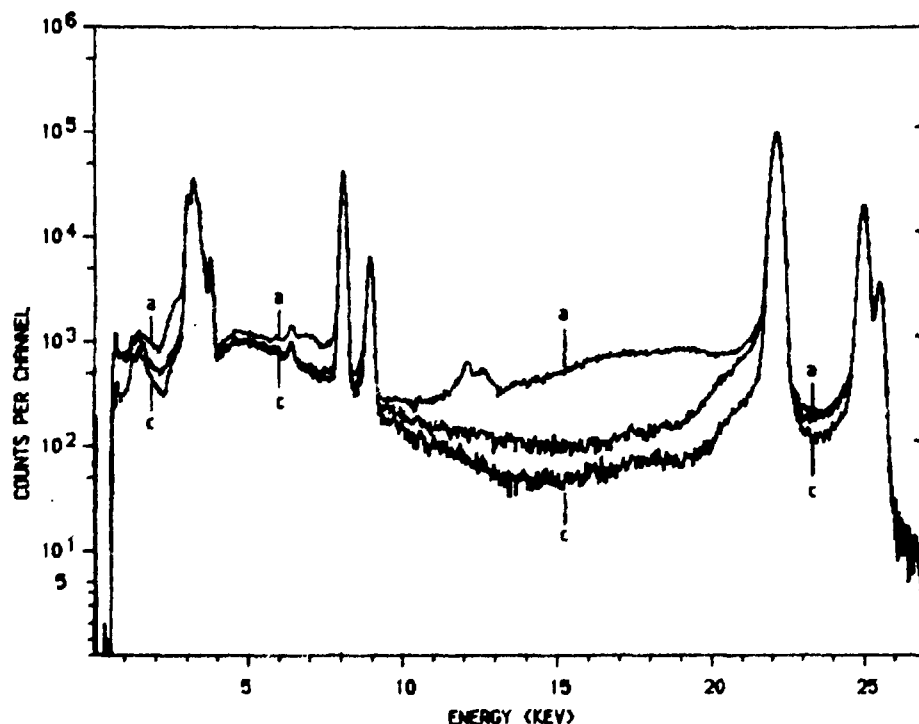


Fig. 5a. X-ray spectra from bombardments of a thick silver plate. The beam diameter was 8 mm and an external X-ray absorber of 340 μ m mylar was used. The total accumulated number of counts is the same in all three cases. In spectrum a, the whole Si(Li) crystal area (about 80 mm²) was exposed to the X-rays and in spectrum b, a tantalum collimator was placed outside the Be-window of the detector thus reducing the effective crystal area to 30 mm². In spectrum c, a temporary further reduction in low energy peak tailing was obtained by removing and immediately reapplying the detector bias.

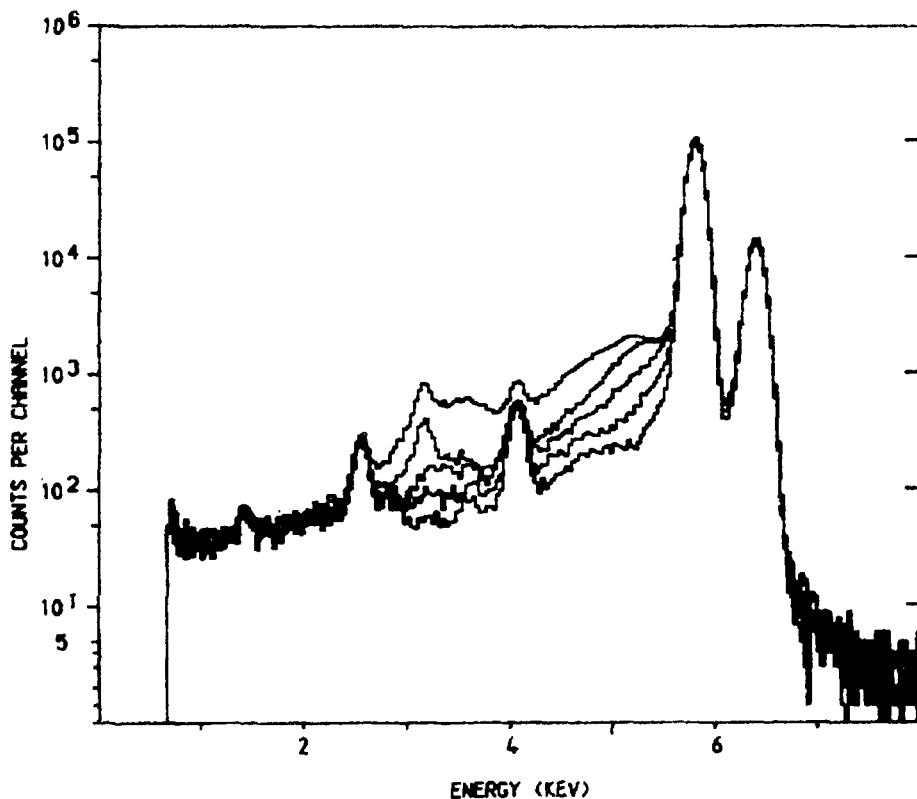


Fig. 5b. Pulse-height spectra from a ^{55}Fe source accumulated at different times after applying the detector bias. The Si(Li) detector was uncollimated and the total numbers of counts in the spectra are the same in all cases. The spectra refer (from bottom to top) to measurements at 0, 20, 60, 120 and 700 minutes after application of the bias.

small collimator is used and thus X-rays only are incident at a small central part ($\approx 10 \text{ mm}^2$) of the sensitive area of the detector, the peak tailing is as low as in case of a recently applied voltage. A tentative explanation for these effects is that, at least for the detector discussed, the on/off-procedure of the detector bias increases the charge collection efficiency in the poor electric field region at the crystal edge. Nothing has been found about this phenomenon in the X-ray detector literature and presumptive customers are advised to pay some attention to this effect when purchasing detectors.

Calibration and detection limits

In ref.¹⁷ the mass calibration of the PIXE system is described in detail. The accuracy in the determination of random elements is estimated to be better than 5% and is still better for ratios of elements. This accuracy refers to the routine analysis of an unknown thin sample.

To check the stability of this mass calibration, a quality control sample has

been run with each batch of samples (≤ 40 samples). By repeated analyses (800 times) of this sample over a year, the long term stability for homogeneous samples is shown to be better than 2.5% and for inhomogeneous samples better than 4% (one S.D.).

Detection limits for PIXE analysis are sensitive to the experimental conditions. To illustrate the capability in routine analysis of the PIXE arrangement described, interference-free mass detection limits were determined in the following way: A thin polystyrene foil (about $30 \mu\text{g}/\text{cm}^2$) was bombarded by a 150 nA proton beam with a diameter of 8 mm. The total accumulated charge was $40 \mu\text{C}$. A $75 \mu\text{m}$ Mylar X-ray absorber was used. The detection limits were calculated as the mass corresponding to $3\sqrt{B}$ pulses, where B is the number of counts in the background within an interval of ± 2 S.D.s around the Gaussian peak (see fig 6).

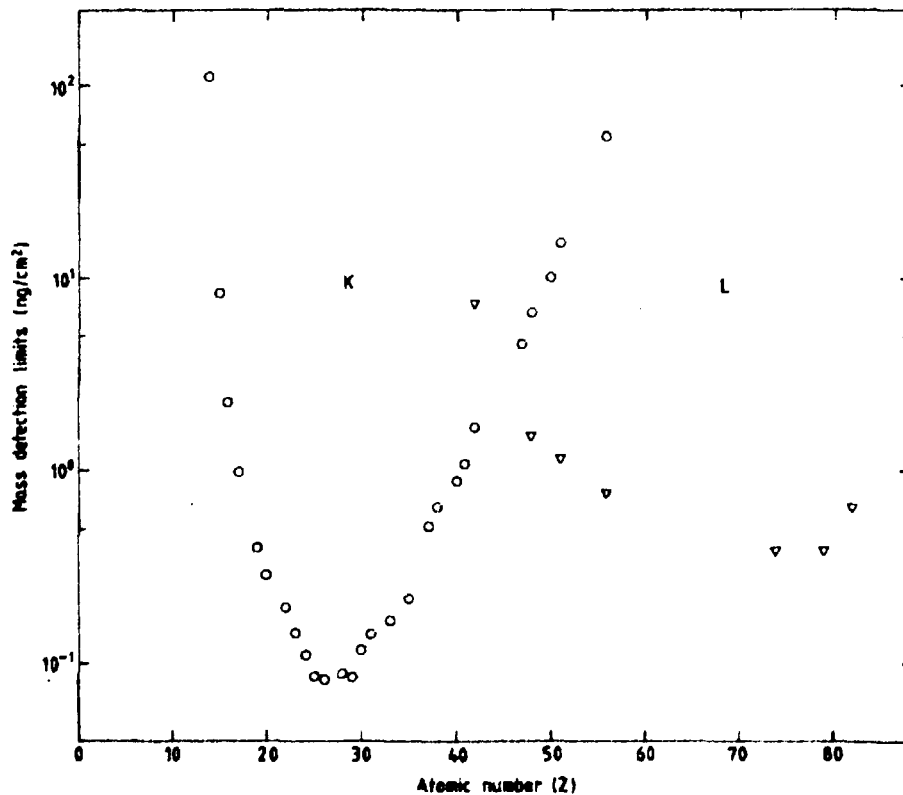


Fig. 6. Experimental mass detection limits versus atomic number calculated assuming no interference between adjacent lines. A 8 mm diameter beam was used to irradiate a thin (about $30 \mu\text{g}/\text{cm}^2$) polystyrene foil with few minor impurities. The total accumulated beam charge was $40 \mu\text{C}$ and an external X-ray absorber of $75 \mu\text{m}$ was used. The detection limits have been calculated as the mass which corresponds to $3\sqrt{B}$ pulses, where B is the background area below ± 2 S.D.s of the Gaussian X-ray peak in question. o and ∇ are determined for K- and L-lines respectively.

FLUORINE ANALYSIS

Physical principles and proton energy

When ^{19}F nuclei are bombarded with protons of MeV energies there is a high cross section for nuclear reactions forming $^{20}\text{Ne}^*$ -nuclei in excited states. The $^{20}\text{Ne}^*$ -nuclei de-excite by alpha particle emission to excited states in ^{16}O , which de-excite promptly to the ground level by the emission of gamma rays with energies 6.13, 6.92 and 7.12 MeV respectively²⁵. Due to the high energy of these gamma rays, they easily penetrate the walls of the irradiation chamber and can be detected by an external gamma ray detector.

The cross section of the $^{19}\text{F}(p,\alpha\gamma)^{16}\text{O}$ reaction as a function of proton energy E_p has a pronounced resonance character²⁶. Very sharp and high resonances for the production of the three gamma rays occur at $E_p = 0.873$ MeV, $E_p = 1.347$ MeV and $E_p = 1.374$ MeV. For E_p in the interval 2.0 to 2.6 MeV the sum of the intensities of these gamma rays (see fig. 7) shows a fairly smooth energy dependence remaining at a high value of cross section and, if the initial proton energy is selected to lie in the 2.0 to 2.6 MeV region and if the protons, after passing the sample, emerge with an energy above 2.0 MeV, the variation in gamma ray yield in the matrix will be less than $\pm 20\%$ (see fig 7). For the integrated matrix yield, the variation is still less and it is rather simple to correct for these small variations if the approximate sample thickness and composition are known. In the proton energy interval from 2.0 to 2.6 MeV the cross sections for proton induced gamma rays in other light nuclides are negligible compared to that in fluorine²⁷ and since the gamma lines (6.13, 6.92 and 7.12 MeV) are virtually free of interfering lines²⁷, the yields from possible competing reactions can be ignored.

Protons with energies of 2 to 3 MeV are the optimal projectiles for PIXE analysis^{28,29,30} and suitable sample thicknesses are up to 1 mg/cm^2 since such samples yield low background radiation and the results do not normally require corrections for particle slowing-down and X-ray absorption. Further, protons in the energy range 2.2 to 2.6 MeV are slowed down less than 0.2 MeV for these sample thicknesses and hence protons in this energy interval can advantageously be used for simultaneous PIXE and fluorine analysis.

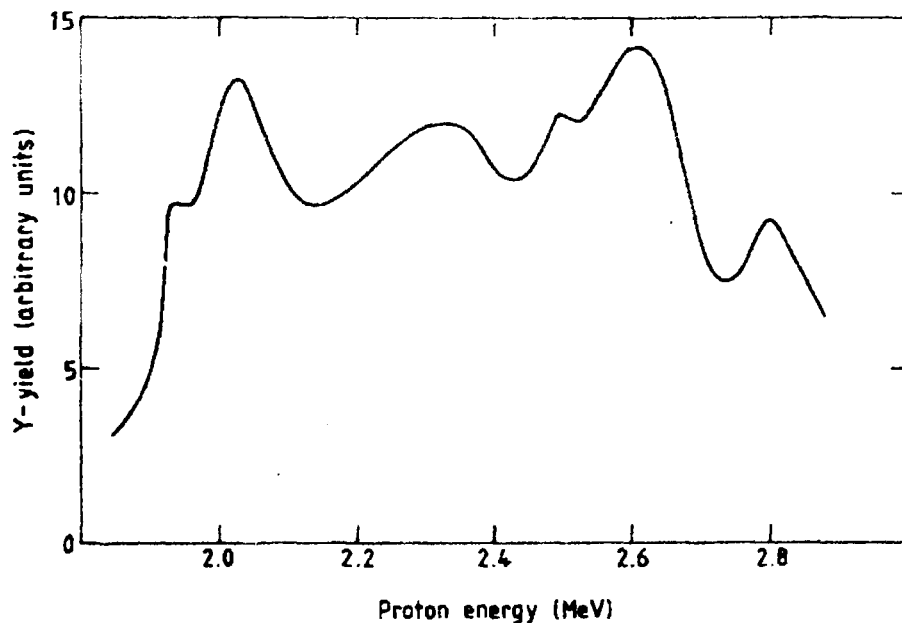


Fig. 7. Yield of high energy gamma rays from the reaction $^{19}\text{F}(p,\alpha)^{16}\text{O}$ in a thin target versus proton energy (after ref.²⁶).

Experimental arrangement

To match the low detection limits possible with PIXE, a large volume detector is preferred for the high energy gamma ray detection. Since no interference of any significance is expected, a large sodium iodide crystal is a good choice.

The practical detection limits are set by the background radiation. The material in collimators, chamber walls, etc., may contain substantial amounts of fluorine and will also be continuously contaminated with fluorine during the bombardment and handling. Since $^{19}\text{F}(p,\alpha)^{16}\text{O}$ reactions take place in the material of the experimental set-up with significant solid angle relative to the detector and since these high energy gamma rays have a high probability of penetrating material on their paths to the detector, their intensities will determine the practical lower limits of detection attainable in a specific analytical system.

Hence, careful design and choice of material is essential to keep the proton induced background radiation low. It is also essential to shield carefully the gamma ray detector from the natural background radiation emanating, e.g. from the concrete walls of the laboratory, since this could otherwise increase the detection limits.

In our set-up 2.55 MeV protons are used and the high energy gamma rays are detected in a 5x4" NaI crystal positioned at a distance of 0.15 m from the

target. Thick (0.06 m) lead shielding is incorporated around the cylindrical detector crystal (see fig 1).

For routine analysis, simple and convenient recording is obtained by a scaler with a lower level discriminator adjusted to count pulses referring to gamma rays produced in the $^{19}\text{F}(p,\gamma)^{16}\text{O}$ reaction only. The discriminator adjustment is carried out using a multi-channel analyser in the gating mode to set the discriminator level just below the double escape peak. The scaler is stopped after a preset accumulated beam charge. The number of counts normalized to the accumulated charge gives a relative yield, Y_s , for the known standard sample with a fluorine content C_s (mass per unit area). The blank substrate which is used to carry the fluorine standard is then irradiated giving another relative yield, Y_{sb} , which is subtracted from Y_s to get the net fluorine yield for the standard. To improve the accuracy of the calibration, several homogeneous standard samples with different fluorine compounds are normally analysed.

The unknown sample, containing the fluorine mass C_u per unit area, is then irradiated similarly to the standard foil, giving a net yield of Y_u . From an analysis of the substrate, Y_{ub} is obtained. Since different samples may be analysed for varying lengths of time and often significantly longer than the standard samples, the influence from natural background radiation should preferably be corrected for as well. This background component is dependent on the collection time and is essentially independent of the accumulated beam charge. Consequently all counts have to be reduced by t times Y_{bt} , where t is the real analysis time and Y_{bt} the number of background events per unit real time. The mass of fluorine per unit area can then be calculated from the following simple formula:

$$C_u = C_s \cdot (Y_u - Y_{ub}) / (Y_s - Y_{sb}),$$

where $C_s / (Y_s - Y_{sb})$ can be the average result from several standard samples. If very high count rates are used, significant electronic dead-time occurs and has to be corrected for.

In our set-up the beam passes through a diffuser foil to permit the analysis of heterogeneous samples. In this foil about 95% of the protons are scattered from their initial direction and out of the beam hitting tube walls and collimators, all of which are more or less contaminated by fluorine. A substantial number of gamma rays will thus be produced here and contribute considerably to the number

of fluorine counts. If, however, a well-focussed beam is used without any diffuser foil (as is possible for homogeneous samples) and deposited in a Faraday cup far away from or well shielded from the NaI crystal (see fig 1), the relative contribution of gamma rays due to scattered protons is significantly reduced. The absolute lower level of detection is then improved by more than one order of magnitude (for this particular experimental configuration).

Performance and Discussion

The samples most commonly analysed at our laboratory are aerosol samples between 0.1 and 1 mg/cm² in thickness. Assuming homogeneous samples it is possible from proton stopping power data³¹ and the yield curve in fig 7 to calculate the integrated relative fluorine gamma ray yield as a function of sample thickness. This function is slowly varying and also slightly smoothed by the energy straggling, which takes place when the protons pass through the matter. The integrated yield from a sample is rather insensitive to the sample composition. In fig 8 the integrated yield of gamma rays from the $^{19}\text{F}(p,\alpha\gamma)^{16}\text{O}$ reaction, without any corrections for straggling, are plotted versus sample thickness for three different matrices for an initial proton energy of 2.55 MeV (corrections for straggling would change the yield less than $\pm 2\%$ over the energy and thickness intervals in question). For samples thinner than 3 mg/cm² a crude

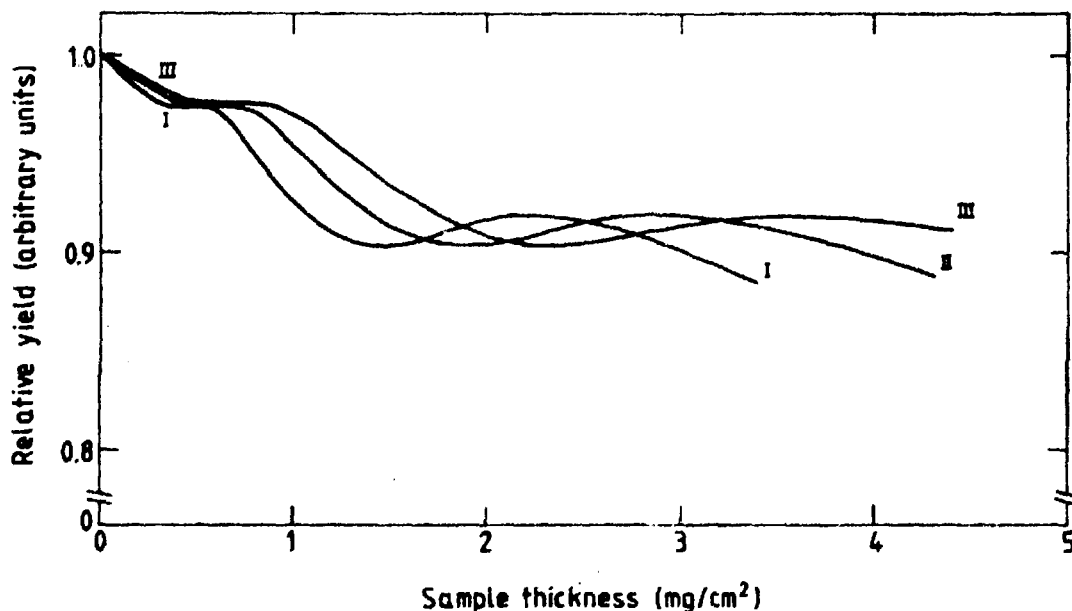


Fig. 8. Integrated relative yield of gamma rays from the $^{19}\text{F}(p,\alpha\gamma)^{16}\text{O}$ reaction versus sample thicknesses for three different matrices: I) 100 % C, II) a welding aerosol matrix composed of 17% O, 20% F, 8% Si, 20% K, 10% Ca, 3% Mn and 22% Fe and III) 100 % Fe. An initial proton energy of 2.55 MeV and homogeneously distributed fluorine have been assumed.

estimation of the sample thickness (better than $\pm 20\%$) and of the sample composition facilitates a simple and accurate correction for sample thickness in fluorine analysis. The accuracy of the correction factor is estimated to be well within $\pm 5\%$. If the sample is not homogeneous, e.g. after sampling an aerosol with time-dependent composition, an estimation can be made from fig 7 to check for possible inaccuracies. Using a proton energy of 2.55 MeV and samples (welding aerosol matrix) thinner than 1 mg/cm^2 with all the fluorine in the first 0.1 mg/cm^2 or in the last 0.1 mg/cm^2 of the sample respectively gives errors of less than $+10\%$ and -10% respectively compared to the assumption of homogeneously distributed fluorine.

The dependence on thickness was checked experimentally by analysis of filters with different loadings of welding aerosols of constant composition. The samples were irradiated by 2.55 MeV protons and the yields normalized to the beam charge collected. In fig.9, the fluorine mass per unit area as determined by the procedure reported is plotted versus the aerosol sample thickness as determined gravimetrically. The circles represent values corrected for the sample thickness of the welding aerosol matrix (see fig 8). If no corrections at all are made, the maximum deviations from the solid straight line in fig 9 will still be less than 10%.

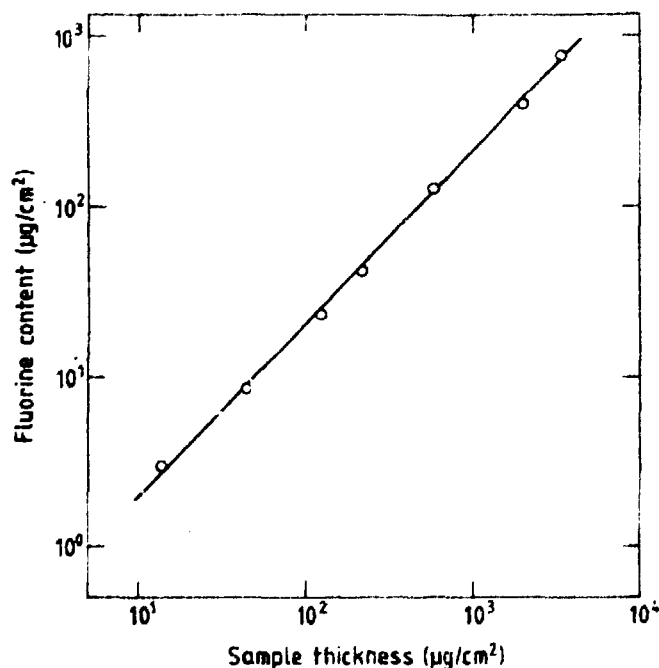


Fig. 9. Fluorine mass per unit area as determined by the $^{19}\text{F}(p,\alpha\gamma)^{16}\text{O}$ method versus the gravimetrically determined sample mass density. Welding aerosol samples of different thicknesses but the same composition (identical to the one in fig 8 II)) were used.

The lower limits of detection for analysis with the $^{19}\text{F}(p,\gamma)^{16}\text{O}$ reaction depend on the probability of producing gamma rays, i.e. on initial proton energy and on sample thickness. Further system parameters, e.g. solid angle and efficiency are important. The detection limits will, however, also be depending partly on the intensity of gamma rays produced outside the sample and strongly on the proton beam characteristics and the surroundings of the beam.

If no diffuser foil is used and the beam is well-focussed so as not to hit the collimators, the absolute mass detection limit is at the same level as those of routine PIXE analyses for heavier elements. By irradiating known masses of a fluorine salt solution pipetted on to Nuclepore filters, the experimental detection limit has in this way been estimated to be 5 ± 3 ng fluorine within the beam area (about 2 mm^2). This rather low detection limit is only applicable to the analysis of homogeneous samples which do not require a homogeneous beam. The detection limit has been defined as the mass corresponding to 3 times the S.D. of the average yield from five blank Nuclepore samples.

For homogeneous beam irradiation, the detection limit is of course more dependent on the geometrical arrangement around the beam and on the shielding of the gamma ray detector. Sample carrying substrates, e.g. filters, vary considerably in thickness and hence the divergence due to multiple scattering when passing through the substrate varies with its thickness. Such scattering of the beam can have a slight influence on the level of background radiation. For routine analysis of samples collected on membrane filters (Nuclepore, thickness: 1 mg/cm^2), the detection limit in this particular set-up has been determined to $100\pm 25\text{ ng/cm}^2$. While being somewhat high compared to PIXE detection limits, this limit is quite sufficient for most applications. In welding aerosol samples, the fluorine mass per unit area is normally 10 to $200\text{ }\mu\text{g/cm}^2$.

The absolute analytical mass determinations are based on a comparison with homogeneous reference fluorine samples of known mass. The accuracy will then depend on the accuracy of the latter samples. The manufacturer states better than 5% accuracy¹⁸ for an individual foil and the accuracy may be further improved by the analysis of several different standard foils and using the average calibration value. In addition to this, errors are introduced because of inaccuracies in the charge integration when irradiating the sample and the standards and because of uncertainties in the corrections for proton slowing-down when the sample's thickness and composition are not accurately

known. The accuracy of the method has been checked experimentally by the analysis of known samples and by comparison with a standard procedure for fluorine analysis.

A very common analytical method for fluorine assaying, e.g. in welding aerosols, is to dissolve the sample followed by determination of the concentration of fluoride ions (F^-) in the solution with a fluoride ion selective electrode³². Only that part of fluorine which is soluble in the solvent used is analysed.

A comparison between the ion selective electrode and the $^{19}F(p,\alpha\gamma)^{16}O$ technique was performed with seven membrane filters, homogeneously loaded with welding aerosols of varying thickness. Each filter was cut in two equal parts, one of which was irradiated with protons and quantified according to the standard foil method described above. The welding aerosol on the second half was dissolved in 20 ml of distilled water and analysed with an ion selective electrode. For higher filter loadings, the solutions were diluted 10 to 25 times before analysis to avoid saturation of the electrode caused by excessive fluoride ion concentrations.

The seven filters (Millipore, diam: 37 mm, pore diam.: $0.8\mu m$) were loaded with amounts from 0.1 to 5 mg of welding aerosol (electrode ESAB OK 48.00) collected on to areas of about 8 cm^2 . A comparison of the results between the two methods of analysis gives an average ratio of $^{19}F(p,\alpha\gamma)^{16}O$ to ion selective electrode results of 1.05 ± 0.04 (\pm one standard error of mean). This is close to unity and within the 5% accuracy for the reference samples stated above. However, the somewhat lower results for the ion selective analysis may be explained by incomplete dissolution of the fluorine from the welding aerosol due to the existence of a fraction of less soluble fluorine compounds. Most fluorine in the fumes from normal low hydrogen coated electrodes is water soluble due to the presence of alkali metals such as Na and K^{33} but sometimes the rather insoluble fluorine compound CaF_2 may also be present in the fume. The $^{19}F(p,\alpha\gamma)^{16}O$ method is not dependent on the chemical form of the fluorine and is further able to analyse nondestructively over a large mass interval. Hence it is very well suited for the analysis of aerosol samples in combination with PIXE analysis.

The precision of the method is mainly determined by the pulse statistics. For a homogeneous sample, the relative standard deviation attained with repeated analyses of the same samples was determined to be 1.5%. The uncertainties due to pulse statistics were less than 0.7%.

Simultaneous X-ray and gamma ray detection

The earlier mentioned possibility of a combination of PIXE and gamma ray detection for fluorine analysis is of great importance. This combination has been tested by irradiation of samples pipetted on to Nuclepore filters. A 1 g/litre stock solution of the salt K_2TiF_6 was used to prepare solutions of known concentrations. Using 5 μ l micro-pipettes, 5 to 20 μ l of the various solutions were pipetted on to filters thus obtaining spot samples with known elemental masses of F, K and Ti. The samples were analysed simultaneously for K and Ti by PIXE analysis and for fluorine according to the technique earlier described. In fig 10 the elemental masses determined are plotted versus masses calculated from known concentrations, volumes and the stoichiometry of the chemical compound. For samples well above the detection limits, the statistical uncertainties due to pulse counting were below 1%. Possible inaccuracies in the sample preparation procedure may account for part of the uncertainty.

The solid line represents the ideal slope 1.00. The correlations between the determined and calculated masses are excellent for all three elements ($r^2 > 0.9997$). For titanium and potassium, the slopes are 0.95 ± 0.01 and 1.02 ± 0.01 respectively and for fluorine 1.08 ± 0.02 (\pm one S.D.). From the error limits given, one can infer that only part of the deviations from the ideal line can be explained by the rather high uncertainties for low elemental masses close to the detection limits. The absence of experimental values for fluorine below 100 ng is due to the absolute mass detection limits being relatively higher than those of PIXE analyses. Although several sources of uncertainty are present, the good accuracy and agreement between the two methods show the analytical combination of PIXE and gamma ray counting for fluorine to be very versatile and powerful extending the analytical capability of the ion beam facility to an important element without increasing irradiation time.

In the section "Detector effects" above, it is shown that problems may occur when X-rays are detected in the Si(Li) crystal if simultaneously an intense flux of MeV gamma rays are incident on the crystal. Consequently, if a very large amount ($> 1 \text{ mg/cm}^2$) of fluorine is present in the sample being analysed, it will be difficult to simultaneously perform PIXE analysis using the procedure described. For the sample thicknesses discussed above ($< 1 \text{ mg/cm}^2$) and normal concentrations of fluorine from below 1% up to a few tens of per cent, this will not be a problem.

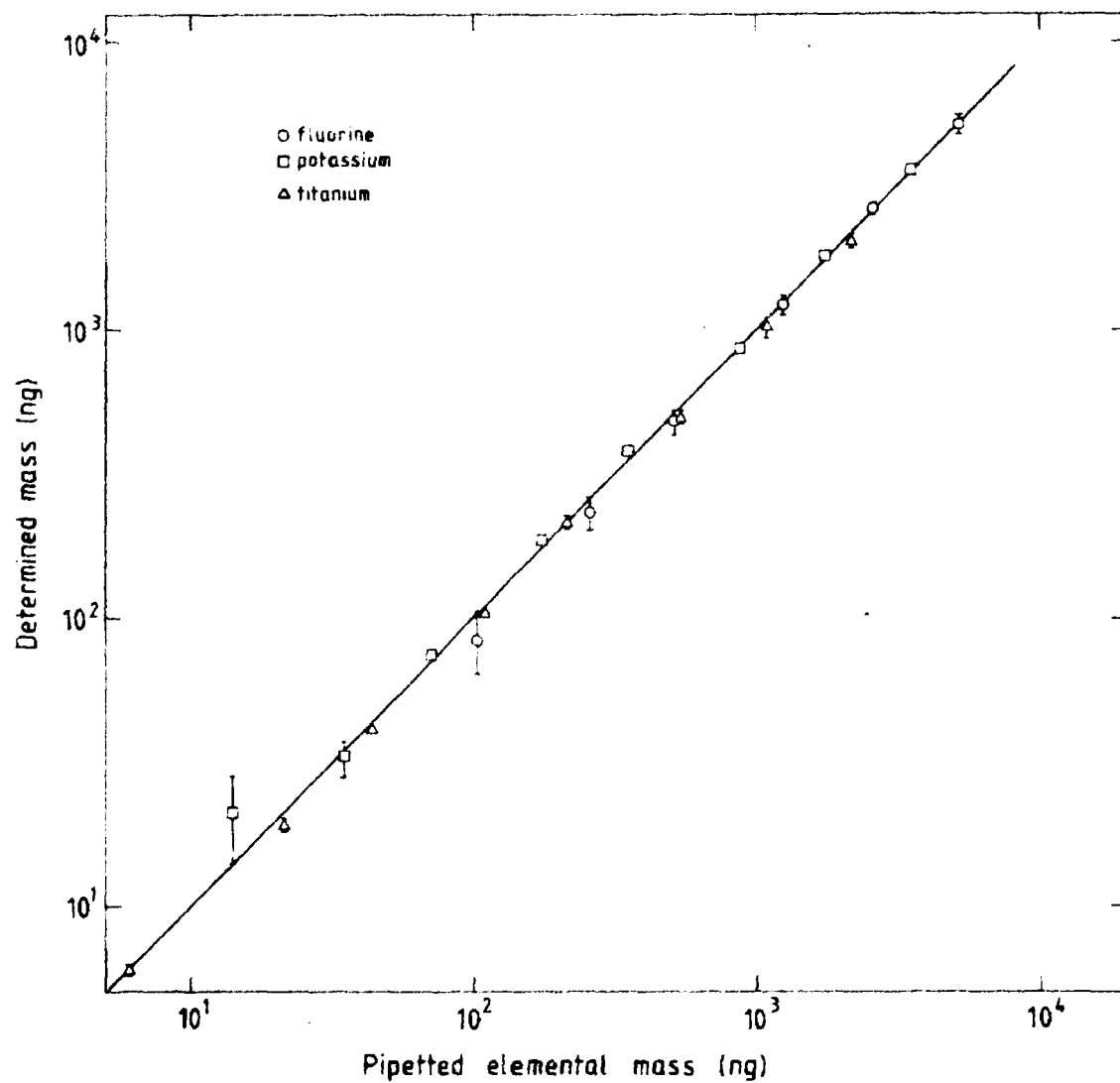


Fig. 10. Elemental masses of potassium and titanium as determined by PIXE and of fluorine as determined by simultaneous use of the $^{19}\text{F}(p,\alpha\gamma)^{16}\text{O}$ method versus the calculated masses of the respective elements. The data points refer to the averages of 5 determinations and the error bars represent \pm one S.D..

CONCLUSIONS

The analytical arrangement developed constitutes an accurate and precise instrument for rapid multi-elemental analyses. Protons with energies of about 2.5 MeV, which in most applications give optimum general sensitivity for PIXE analysis, can be used for simultaneous and simple analysis of fluorine in thin samples ($<1 \text{ mg/cm}^2$) by detecting the high energy gamma rays from the reaction $^{19}\text{F}(p,\alpha\gamma)^{16}\text{O}$.

The irradiation chamber comprises an automatic sample changing system based on commercial slide frames, externally exchangeable X-ray absorbers and proton beam collimators, on-demand beam pulsing, beam diffuser foil and an electron emitting carbon filament for charge build-up reduction. Careful mass calibration and testing of the different components have been carried out and the set-up shows good overall performance and long term stability.

The impact of protons and intense fluxes of MeV gamma rays on the X-ray detector give distorted X-ray spectra. To avoid proton impact, a rather thick (110 μm) Be-foil is used as chamber window. To improve the X-ray spectra, the Si(Li) crystal has been collimated from 80 mm^2 to 30 mm^2 effective sensitive area thus reducing low energy peak tailing due to incomplete charge collection. Removing and reapplying the detector bias reduces low energy tails of X-ray peaks temporarily.

From comparisons with a standard method for fluorine analysis (ion selective electrode) and proton irradiation of samples with known masses of fluorine, potassium and titanium, it can be inferred that counting the gamma rays from the $^{19}\text{F}(p,\alpha\gamma)^{16}\text{O}$ reaction is an accurate and precise technique for fluorine analysis of thin samples, e.g. in aerosol samples, and that it can preferably be combined with simultaneous PIXE analysis.

ACKNOWLEDGEMENTS

The contributions of the following individuals to the work presented here is gratefully acknowledged:

R. Hellborg, K. Håkansson and C. Nilsson have been responsible for the excellently well-maintained accelerator laboratory at which this work has been carried out. The mechanical constructions were skilfully built by K. Sjöberg, P.

Jensen and L.-B. Nilsson and several of the electronic units were designed and built by E. Karlsson.

Finally, we are grateful to the members of the PIXE research group³⁴ in Lund for many stimulating and lively discussions and for valuable contributions to this work.

REFERENCES

1. T.B. Johansson, R. Akselsson and S.A.E. Johansson, Nucl. Instr. and Meth., 84 (1970) 141.
2. Proc. Int. Conf. on Particle Induced X-Ray Emission and its Anal. Applic., Nucl. Instr. and Meth., 142 (1977).
3. Proc. Sec. Int. Conf. on Particle Induced X-Ray Emission and its Anal. Applic., Nucl. Instr. and Meth., 181 (1981).
4. J.W. Nelson and D.L. Meinert, Adv. X-Ray Anal., 18 (1975) 598.
5. T.A. Cahill, in New Uses of Ion Accelerator, Ed. J.F. Ziegler, Plenum Press. (1975) 1.
6. R.D. Lear, H.A. Van Rinsvelt and W.R. Adams, Adv. X-Ray Anal., 19 (1976) 521.
7. R.B. Boulton and G.T. Ewan, Anal. Chem., 49 (1977) 1297.
8. L.-E. Carlsson and K.R. Akselsson, Nucl. Instr. and Meth., 181 (1981) 531.
9. K.G. Malmqvist, G.I. Johansson, M. Bohgard and K.R. Akselsson, Nucl. Instr. and Meth., 181 (1981) 465.
10. E. Møller and N. Starfelt, Nucl. Instr. and Meth., 50 (1967) 225.
11. J.W. Mandler, R.B. Moler, E. Raisen and K.S. Rajan, Thin Solid Films, 19 (1973) 165.
12. K. Ishi, S. Morita and H. Tawara, Phys. Rev. A, 13 (1976) 131.
13. M. Ahlberg, G. Johansson and K. Malmqvist, Nucl. Instr. and Meth., 131 (1975) 377.
14. K.G. Malmqvist, E. Karlsson and K.R. Akselsson, to be published.

15. H.C. Kaufmann, K.R. Akselsson and W.J. Courtney, Nucl. Instr. and Meth., 142 (1977) 251.
16. G.I. Johansson, to be published.
17. G.I. Johansson, J. Pallon, K.G. Malmqvist and K.R. Akselsson, Nucl. Instr. and Meth., 181 (1981) 81.
18. J.A. Heagney and J.S. Heagney, Nucl. Instr. and Meth., 167 (1979) 137.
19. T.A. Thornton and J.N. Anno, J. Appl. Phys., 48 (1977) 1718.
20. R. Akselsson and T.B. Johansson, Nucl. Instr. and Meth., 91 (1971) 663.
21. L. Meyer, Phys. Stat. Sol., 44 (1971) 253.
22. R. Nobile, Y. Civelekoğlu, P. Povh, D. Schwalm and K. Traxel, Nucl. Instr. and Meth., 130 (1975) 325.
23. F. Folkmann, J. Phys. E, 8 (1975) 429.
24. F.S. Goulding, J.M. Jaclevic, B.V. Jarrett and D.A. Landis, Adv. X-Ray Anal., 15 (1972) 470.
25. R. Hellborg and L. Ask, Physica Scripta, 6 (1972) 47.
26. H.B. Willard, J.K. Bair, J.D. Kington, T.M. Hahn, C.W. Snyder and F.P. Green, Phys. Rev. 85 (1952) 849.
27. I. Golicheff, M. Loeuillet and Ch. Engelmann, J. Radioanal. Chem. 12 (1972) 233.
28. S.A.E. Johansson and T.B. Johansson, Nucl. Instr. and Meth., 137 (1976) 473.
29. A.W. Herman, L.A. McNelles and J.L. Campbell, Int. J. of Appl. Radiat. and Isot., 24 (1973) 677.

30. B. Raith, M. Roth, K. Göllner, B. Gonsior, H. Ostermann and C.O. Uhlhorn, Nucl. Instr. and Meth., 142 (1977) 39.
31. L.C. Northcliffe and R.F. Schilling, Nucl. Data Tables, A7 (1970) 233.
32. P.L. Bailey, "Analysis With Ion-Selective Electrode", Heyden, London (1976).
33. M. Pantůček, Am. Ind. Hyg. Ass. J., 32 (1971) 687.
34. Except for the authors the Lund PIXE group comprises the following individuals: M. Bohgard, L.-E. Carlsson, H.-C. Hansson, E.-M. Johansson, S.A.E. Johansson, H. Larnefors, Li Hung-Kou and J. Pallon.